A long-term context (931-2005 C.E.) for rapid warming over central Asia

Davi NK[1&2], D'Arrigo R[1], Jacoby GC[1], Cook ER[1], Anchukaitis K[3], Nachin B[4], Rao MP[1&5], and Leland C[1&5]

Keywords: Paleoclimate, Temperature, Tree-Ring, Mongolia, Reconstruction

[1] Tree-Ring Laboratory, Lamont-Doherty Earth Observatory, 61 Route 9W Palisades, New York 10964, USA

[2] Department of Environmental Science, William Paterson University, Wayne NJ, 07470

[3] Dept. of Geology and Geophysics, Woods Hole Oceanographic Institute, Woods Hole MA, 02543

[4] National University of Mongolia 14201 Ulaanbaatar, Mongolia 46A/135

[5] Department of Earth and Environmental Science, Columbia University in the City of New York, NY, U.S.A. 10027

Corresponding Author: Nicole Davi, ndavi@ldeo.columbia.edu, 201-446-8417

Abstract Warming over Mongolia and adjacent Central Asia has been unusually rapid over the past few decades, particularly in the summer, with surface temperature anomalies higher than for much of the globe. With few temperature station records available in this remote region prior to the 1950s, paleoclimatic data must be used to understand annual-to-centennial scale climate variability, to local response to large-scale forcing mechanisms, and the significance of major features of the past millennium such as the Medieval Climate Anomaly (MCA) and Little Ice Age (LIA) both of which can vary globally. Here we use an extensive collection of living and subfossil wood samples from temperature-sensitive trees to produce a millennial-length, validated reconstruction of summer temperatures for Mongolia and Central Asia from 931 to 2005 CE. This tree-ring reconstruction shows general agreement with the MCA (warming) and LIA (cooling) trends, a significant volcanic signature, and warming in the 20th and 21st Century. Recent warming (2000-2005) exceeds that from any other time and is concurrent with, and likely exacerbated, the impact of extreme drought (1999-2002) that resulted in massive livestock loss across Mongolia.

Keywords: Mongolia, temperature, tree-ring, dendrochronology, reconstruction, global warming

1 Introduction

Our understanding of long-term temperature variability and its causes is extremely limited in remote Central Asia, due to short and sparse meteorological data, as well as a paucity of long-term, high-resolution, temperature-sensitive proxy records. Instrumental records, typically only reaching back to the 1940s or later, show that temperatures in central Asia have been increasing rapidly, particularly since the mid 1990's, and are currently warmer then at any other time in recorded history (Chen et al. 2009). Paleoclimate reconstructions, largely derived from tree-ring records, have been used to extend our understanding of temperature across Mongolia and central Asia (Jacoby et al. 1996, D'Arrigo et al. 2000, D'Arrigo et al. 2001a) on long-term scales. Among the existing temperature tree-ring records from central Asia, few extend back to the early Medieval Climate Anomaly (MCA, ca. 850–1050 C.; Lamb 1965, see Cook et al. 2013). The regional chronology thus far, from Solongotyn Davaa, in Mongolia's central Tarvagatay Mountains, extends back to 262 C.E., based on living and subfossil wood of Siberian pine (D'Arrigo et al. 2001a). However, this long record could not be used to generate calibrated and validated reconstructions, due to the limits of nearby meteorological station records. These cover only a few decades, are situated at lower elevations, and are quite distant from the tree-ring sites.

Here, we develop a millennium-length (931-2005 C.E.) tree-ring chronology from larch trees (*Larix sibirica*) growing at elevational treeline sites in Mongolia, where the dominant limiting factor for growth is temperature (Jacoby et al. 1996; D'Arrigo et al. 2000, 2001a&b). The chronology and reconstruction, from a site named Ondor Zuun Nuruu (OZN; meaning ' High East Ridge'), has an unusually large sample depth (> 200 samples) and can be calibrated and validated using regionalized meteorological data from Mongolia and Russia. The reconstruction allows us to evaluate temperature variability and extremes over the past millennium in central Asia, a region that is warming faster then many places on Earth (Chen et al. 2009). It also places recent warming trends into a long-term context, contributes to our understanding of spatial patterns of the MCA and LIA, and provides evidence of significant volcanic influence on Central Asia temperature.

2 Materials and methods

2.1 Instrumental data

The OZN tree-ring site is located just west of Lake Hovsgol, in north central Mongolia near elevational treeline (2400m, **Figure 1**), and is in one of the coldest regions in central Asia. Instrumental temperatures from Rinchinlhumbe (**Table 1**), the nearest station to the OZN site (~50km away), average -29°C in winter (DJF), and 12°C in the summer (JJA), typical of the extreme continentality of central Asia. We estimate that temperatures at the OZN site are between ~6°C and ~9°C colder then the Rinchinlhumbe site (~900 meters lower) based on adiabatic lapse rates. The Rinchinlhumbe station record only begins in 1974, however, and there are few long temperature records from this region. To the north of OZN in Russia, station records reach as far back as the late 1800s at Minusinsk and into the 1830s at Irkutsk (**Figure 1, Table 1**). In Mongolia, the nearest and most complete station records are for Bulgan and Muren (1941-2011), both relatively high elevation sites (>1200M), and more similar to the higher elevation OZN treeline site. We thus generated a regional temperature record by averaging the data from Irkutsk, Minusinsk, Muren and Bulgan. Mean average June-July temperatures from Mongolia (Bulgan & Muren), and Russia (Irkutsk & Minusinsk) correlate at $r=0.5$ ($p< 0.05$) over the 1941-2005 period. Nine missing monthly values in the station data were replaced with monthly averages. Gridded temperature data from the Climate Research Unit (CRU TS 3.10, Harris et al. 2013) was also evaluated in order to compute spatial correlations of temperature with the reconstruction.

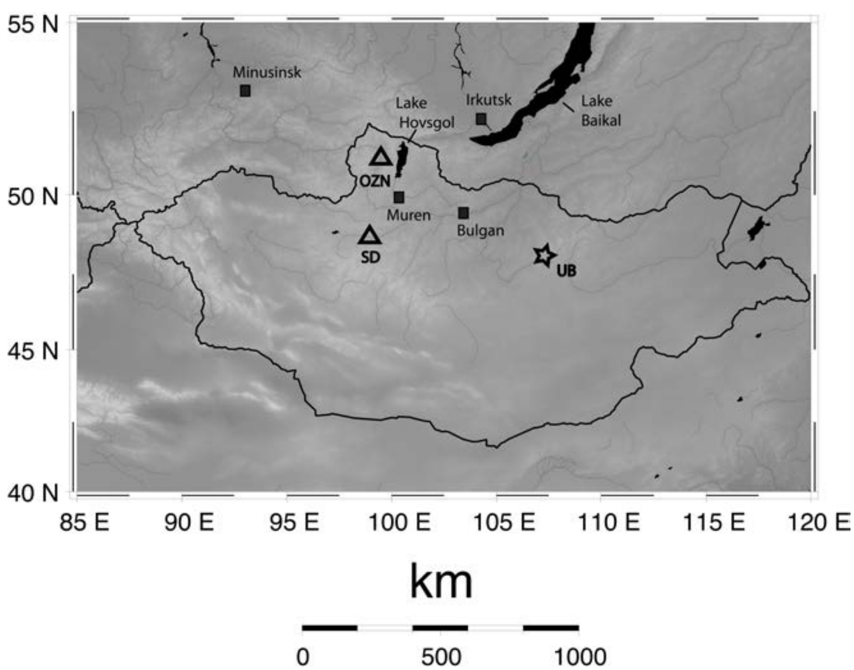

Figure 1. Map showing the location of OZN and Sol Dav sites (triangles), the four meteorological stations (squares), and the capital of Mongolia Ulaanbaatar (star). Greyscale shows elevation with higher areas in lighter colors. Lakes are labeled and shaded in black. The Rinchinlhumbe station is located within the OZN triangle.

	Coordinates	**Elevation**	**span**
Irkutsk*	52.27N, 104.32E	469m	1820-2011
Muren*	49.57N, 100.17E	1283m	1941-2011
Bulgan*	48.80N, 103.55E	1208m	1941-2011
Minusinsk*	53.70N, 91.70E	254m	1886-2011
Rinchinlhumbe	51.12N, 99.67E	1583m	1974-2011

* used for modeling

Table 1. Meteorological station coordinated, elevation and time-span.

2.2 Tree-ring data

The OZN tree-ring site is located near elevational treeline (2400m) on a west-facing slope of large granite slabs with pockets of soil, abundant moisture, and shallow or perched water table. Larch trees grow primarily on soil "islands" amidst the granite-boulder talus. Similar to Sol Dav (D'Arrigo et al. 2001a), OZN is an open canopy site and alpine shrubs and grasses grow near the trees, an indication of mesic conditions. These microsite features all indicate that temperature is likely to be the primary factor limiting tree growth at OZN. These trees are extremely slow-growing and long-lived. One living tree dated back to 1405 and had a diameter of roughly 36 cm (indicating an average annual growth of only ~0.3 mm per year). There were also abundant relict logs scattered throughout the site. All living trees were sampled non-destructively by coring, and cross-sections or cores were taken from dead trees. Sample depth at this site is substantial, with a total of 209 samples collected, over half (133) coming from subfossil wood.

Ring-width series were detrended using Signal Free (SF) and Regional Curve Standardization (RCS) procedures (Melvin and Briffa 2008), which aid in the preservation of long-term, centennial scale variability in excess of the segment lengths of the individual tree-ring series being processed (Cook et al. 1995). Prior to SF-RCS detrending, adaptive power transformations were applied to the ring-width measurements (Cook and Peters 1997). Doing so stabilizes the variance of the ring-width series and protects the resulting detrended indices from potential inflationary bias, especially at the outer end of the chronology. See Cook and Peters (1997) for details. The RCS curve itself was estimated by aligning and averaging all tree-ring data by biological age and fitting a smooth time-varying spline to the average (Melvin et al. 2007). The resulting smoothed RCS curve was then used to detrend each individual power-transformed ring-width series and the resulting residuals were averaged into a mean chronology after the data were re-aligned to their original calendar years. In the iterative signal free version of RCS used here, the final SF-RCS chronology converged after 3 iterations, after which there was no meaningful change in the SF-RCS chronology. See Melvin & Briffa (2013) for procedural details of the method.

The resulting SF-RCS chronology spans from 715 to 2005 CE, with a mean segment length of 348 years for all series. We truncated the chronology at the year 931, when sample depth drops below six series and three trees. The Expressed Population Signal (EPS; Cook and Kairiukstis, 1990) measures the strength of the common signal for a set of tree-ring series in a given chronology. EPS remains at 0.84 or above throughout the period 931-2005. Generally a level of 0.85 or above is considered a common but arbitrary threshold (Wigley et al. 1984), although should not be interpreted rigidly. RBAR, the mean correlation between tree-ring series, a measure of common variance or signal strength, ranged from 0.37 to 0.73, with a mean of 0.49.

2.3 Superposed Epoch Analysis

We investigated the presence of a volcanic cooling signal in the OZN reconstruction using Superposed Epoch Analysis (SEA, Haurwitz and Brier 1981). Two methods of significance testing - random sampling and block reshuffling, were used to assess statistical significance given the presence of tree-ring autocorrelation (Adams et al. 2003). Ring width indices in particular can have a significant year-to-year autocorrelation due to persistent biological influences following growing season conditions (D'Arrigo et al 2013), which can affect the detection of volcanic signals in tree rings. In both cases, the number of Monte Carlo iterations applied was 10,000. The SEA is performed by normalizing the data by the mean of the pre-event years. We generated two different volcanic event year lists using estimates of volcanic forcing during the last millennium, from Gao et al. (2008) (1177 1214 1259 1276 1285 1342 1453 1601 1642 1763 1810 1816 1836 1992) and Crowley et al. (2008) (1229 1258 1286 1456 1600 1641 1695 1809 1815 1884 1992), because of uncertainty in the timing and magnitude of past explosive volcanism (Schmidt et al. 2012). We created these event year lists by querying the forcing series for years with negative forcing of at least the magnitude of the Pinatubo (1991) eruption, and then using only the first year if there were multiple consecutive years with large negative forcing (i.e. for 1258, this means using 1258 from the Crowley et al. (2008) data and not 1259 and 1260). We note that Krakatoa is missing from the Gao et al. (2008) event list because it is smaller in magnitude (-1.62912 w/m^2) than Pinatubo (-2.48151 w/m^2) in the global annual compilation from Schmidt et al. (2012), and therefore didn't meet our a priori criteria.

3 Results

Correlation coefficients were calculated between the OZN chronology and monthly instrumental temperature records for the region **(Figure 2**). Temperature was always positively correlated with tree-growth indicating that warmer temperatures enhanced growth. Since the strongest positive correlations were consistently found with current June and July temperatures, we averaged June and July values from the four nearest and most complete stations as described above (**Table 1**). As expected, based on site characteristics, we did not find any significant correlation between tree growth and precipitation using the Muren station precipitation data.

We used the SF-RCS chronology as the predictor and the regionalized station temperature data as the predictand in a principal component regression (Cook et al. 1994) to produce a summer temperature reconstruction for the past 1075 years. To evaluate the fidelity of the model a split calibration/validation method was used on both the 1941-1973 and 1974-2005 periods. The reconstruction has significant skill, based on the Reduction of Error (RE), and Coefficient of Efficiency (CE) statistics (Cook and Kairiukstis, 1990) (**Table 2**). The reconstruction explains 43% of the variance in the instrumental series and captures the year-to-year variations in the regionalized station data over the common period (**Figure 3a**). A model based on longer records from Russia alone (1886-2011) did not validate and neither did validation on the Russian records using early 20th Century data (1910-1940). This result is not surprising considering the considerable distance between the OZN site and the Russian stations, and their differences in elevation, illustrating the difficulty in creating and need for high-resolution proxies such as tree rings in such remote regions.

A comparison of the OZN temperature reconstruction with CRU gridded summer temperatures (**Figure 4**) reveals the spatial extent of the relationship between tree growth and temperature — significant correlations cover a sizeable area of central Asia ($p<0.1$). We also tested the model by averaging gridded CRU TS3.10 data from 95-105°E and from 47-53°N. Results were similar (variance explained = 41%, $p< 0.01$), but slightly lower then the model based on the averaged station data (variance explained = 43%, p< 0.01). We did not test the earlier portion of the gridded data (1901-1940) because the underlying station data that is used to develop the gridded CRU data is extremely sparse during this time.

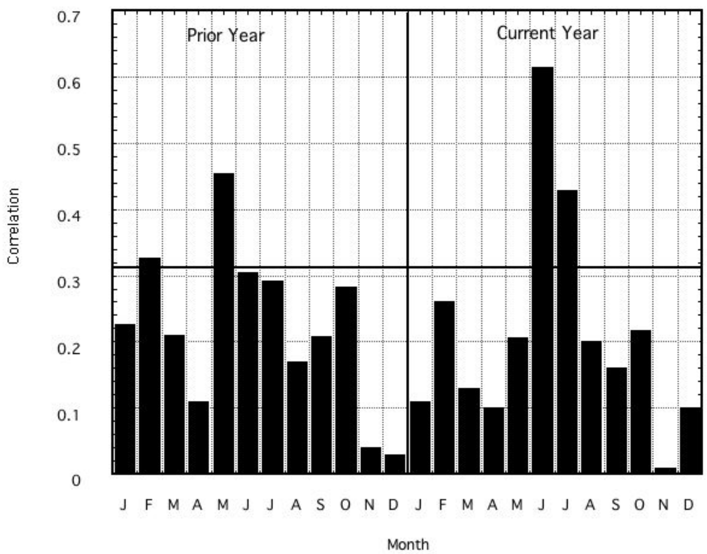

Figure 2. Monthly correlation coefficients over 24 months (verticle bar shows prior year and current year) of the OZN chronology with averaged station data from four stations from Mongolia (Bulgan & Muren), and Russia (Irkutsk & Minusinsk) over the 1941-2005 common period. The Black horizontal bar = the 95% confidence level.

	Calibration 1941-1973	Validation 1974-2005	Calibration 1974-2005	Validation 1941-1973
RE	0.340	0.456	0.551	0.327
CE	0.340	0.448	0.551	0.270
PR	0.583	0.742	0.742	0.629

Table 2. Calibration and validation statistics. RE is the reduction of error, CE is coefficient of efficiency (Cook and Kairiukstis, 1990) and PR is Pearson's correlation coefficient. RE and CE are measures of shared variance between the actual and modeled series. In the calibration period, RE and CE are identical to the coefficient of determination R^2. Values above zero indicate that the regression model has skill.

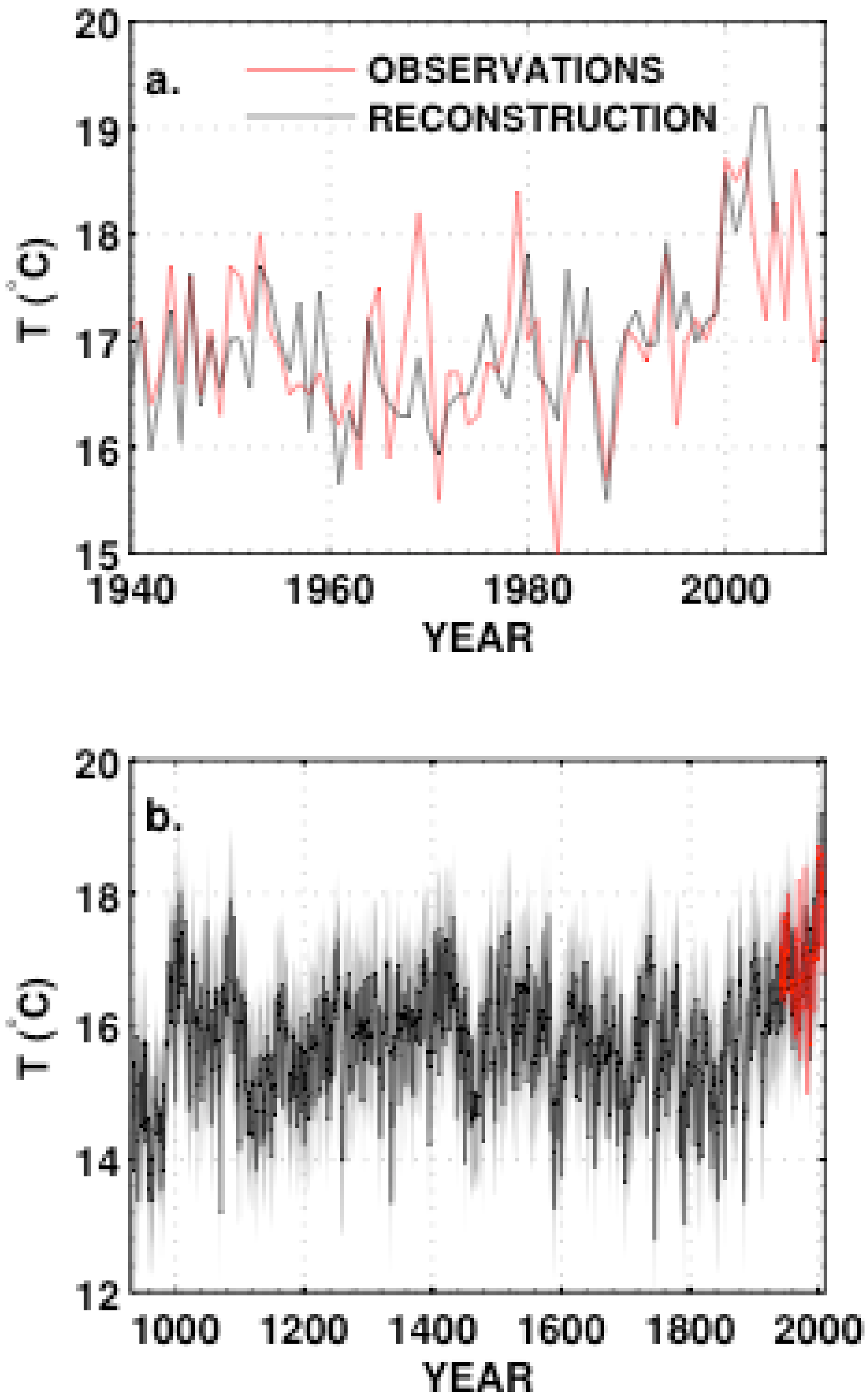

Figure 3. **a.** Observed average June-July station temperature data (red) with the tree-ring based reconstructed data (black), and **b.** Northern Mongolia summer temperature reconstruction spanning 931-2005, with the observed record in red and Error envelope on panel b is plus/minus 2 root mean square error.

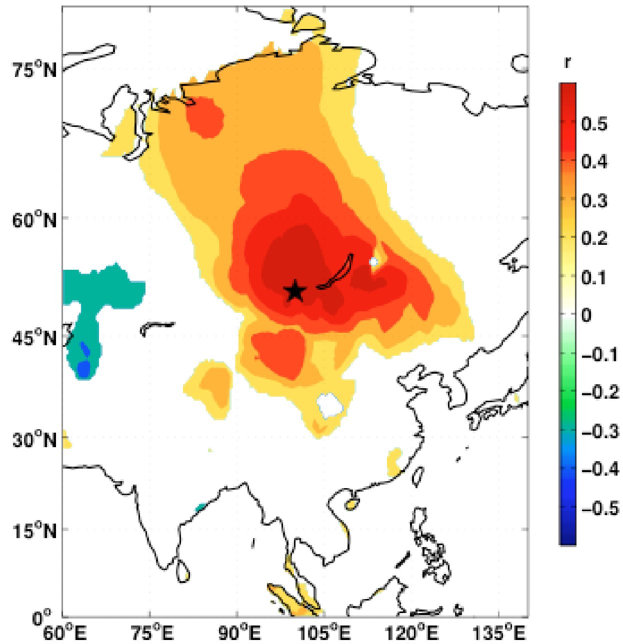

Figure 4. Spatial correlation map of the OZN chronology with CRUTS3.10 average June-July temperatures from 1941-2005. The linear trend was determined and subtracted from all data prior to correlating variables. For grid point data, the linear trend is subtracted from each grid point individually from all data. A similar but weaker pattern emerges using CRU data from 1901-1940 (not shown), however the underlying data is remarkably sparse. The OZN site location is marked by a star.

4 Discussion

4.1 Variability through time:

The reconstruction reveals considerable variability through time on annual to multidecadal and longer time scales (**Figure 3b)**, including sustained warm and cold episodes that broadly coincide with the MCA and LIA epochs as described elsewhere for this region (Cook et al. 2013). Reconstructed summer temperatures range from 12.8-19.2 °C. The coldest, sustained multi-decadal epoch occurred in the 900s when temperatures remained below the long-term mean (15.8° C) for 50 years from 934-984 (**Figure 3b)**. This severe cold period was followed by rapid warming from 996-1015 and again from 1074-1093. These latter periods are the 3rd and 6th warmest 20-year periods (respectively) in the entire record (**Table 3**). Warmth generally persisted until nearly the end of the 1000s. This period (~ 900 to 1100) coincides with the MCA, which has been described in other proxy records for Asia (Ge and Wu 2011, Cook et al. 2013), elsewhere across the Northern Hemisphere (Diaz et al. 2011) and the globe (Cook et al. 2002) but has been shown to vary spatially and temporally (Mann et al. 2009, PAGES 2K Consortium 2013). 20th and 21st Century warming is higher then at any other time in the reconstruction. Mean reconstructed temperature from 990 to 1090 (the warmest part of the MCA) is 16.2°C compared to 16.7°C from 1905 to 2005. By comparison, average summer reconstructed temperature from 1999 to 2004 is 18.4°C, and the 1st (1986-2005, 17.5°C), 2nd (1941-1960, 16.9°C) and 5th (1966-1985, 16.7°C) warmest non-overlapping 20-year-periods occur in the 21st and 20th Century. The 3rd (996-1015, 16.9°C) and 4th (1412-1431, 16.7°C) warmest non-overlapping 20 year periods occurred during the MCA.

Another multi-decadal cold period began in 1111 with temperatures largely below average until 1155. 1111-1130 and 1135-1154 are the 4th and 8th coldest 20-year periods in the reconstruction, respectively. A warming trend followed and lasted nearly 300 years, peaking with warmth from 1412-1431 (the 4th warmest 20 year period on record) that is nearly comparable with the MCA and 20th century warming. Cold conditions are generally observed during the LIA epoch from ~1350 to 1880, particularly from 1454-1473 (9th coldest 20 year period), 1584-1603 (5th coldest), 1695-1714 (6th coldest), 1792-1801 (7th) and 1832-1851 (2nd). From 1832-1851 average summer temperatures were ~14.5°C with cold temperatures persisting for more then two decades—from 1830 until 1854.

After the mid-1800s cold, temperatures began to warm and continuing until the end of the record in 2005. Attributed to anthropogenic forcing (Masson-Delmotte et al. 2013), this warming reflects similar trends found in both recorded and paleoclimatic data from around the Northern Hemisphere (e.g. Jacoby et al. 1996, Cook et al. 2004; 2013, D'Arrigo et al. 2006, Juckes et al. 2007, PAGES 2K Consortium 2013, Masson-Delmonte et al. 2013). In fact, seven of the ten warmest individual years and five of the warmest 20-year periods (**Table 3**) occur in the 20th and 21st Century. The warmest 20 year period, 1986-2005, has an average summer temperature of 17.5°C relative to a long term mean of 15.8 °C. The 20th Century has the highest century-scale average temperatures over the length of the reconstruction, with the MCA not far behind (**Table 4**).

The unusually warm reconstructed temperature anomalies in the years 2003 and 2004 are consistently observed across all living tree samples as enhanced growth. There was no ecological evidence of disturbance such as logging or fire at the study site. These anomalies follow three of the warmest summers on record (2000-2002), which likely benefited radial growth as well.

A. Warmest

	1-yr	3-yr	20-yr
1	2003	2002-2004	1986-2005
2	2004	1999-2001	1941-1960
3	2000	1084-1086	996-1015
4	2002	1994-1996	1412-1431
5	2005	1007-1009	1966-1985
6	2001	1953-1955	1074-1093
7	1007	1518-1520	1891-1910
8	1994	1984-1986	1725-1744
9	1086	1420-1422	1921-1940
10	1008	1738-1740	1511-1520

B. Coldest

	1-yr	3-yr	20-yr
1	1746	963-965	956-975
2	1792	942-944	1832-1851
3	1071	1842-1844	932-953
4	1589	959-961	1111-1130
5	1336	979-981	1584-1603
6	1884	1259-1261	1695-1714
7	965	1589-1591	1792-1801
8	943	1699-1701	1135-1154
9	959	1336-1338	1454-1473
10	1843	1884-1886	1186-1205

Table 3. Warmest/coldest non-overlapping period table:

931-999	15.02
1000-1099	16.14
1100-1199	15.32
1200-1299	15.78
1300-1399	15.96
1400-1499	15.95
1500-1599	15.94
1600-1699	15.66
1700-1799	15.57
1800-1899	15.57
1900-1999	16.60

Table 4. Century-scale average temperature in °C.

4.2 Comparison to other records:

There are relatively few tree-ring proxy records for temperature in Mongolia. Four temperature sensitive alpine tree-line records were produced by D'Arrigo et al. (2000) that dated back to 1450 and reflected regional and Northern Hemisphere scale temperature variations. Of those, one site (Sol Dav) was revisited to sample 'relict' wood that resulted in a temperature sensitive chronology dating back to 262CE (D'Arrigo et al. 2001a). More recently, a large network of tree-ring chronologies was used to reconstruct summer temperature for temperate East Asia, north of 23°N (Asia2K, Cook et al. 2013) from 800-1989. The four chronologies from D'Arrigo et al. (2000 & 2001a) were used as part of that large-scale reconstruction along with 418 other chronologies as potential predictors.

The OZN and Sol Dav records correlate significantly (r= 0.5, $p<0.05$) over the 900-1999 common period and all three reconstructions have good agreement prior to the late 1300s (**Figure 5**). The OZN reconstruction shows that the warm early MCA occurred from ~990 to 1110 in Northern Mongolia. This MCA warm period is consistent with the Asia 2K record, but not the Sol Dav record (**WI- Figure 5**). Sol Dav shows considerably more warming (inferred) beginning in the 900s. The period from ~1110 to 1160 is a very cold period for Sol Dav, OZN, and Asia 2K (**CI – Figure 5**) and is followed by a general warming trend in OZN that peaks in the early 1400s that is seen in all three records (**WII-Figure 5**). Very cold temperatures occur in all three records from the 1450s to the 1470s (**CII-Figure 5**), and again from the late 1500s to the early 1600s (**CIII-Figure 5**). During the 19th Century, all records show cooling in the mid 1800s (**CIV-Figure 5**). Sol Dav has much less growth (inferred cooling) then OZN from ~1800 to 1910. A warming trend consistent with global temperature patterns begins in the 1850s at OZN, 1870s at Sol Dav and 1880s in the Asia2K reconstruction and continues for the remainder of the record (**WIII-Figure 5**). Since 1999, to the end of the OZN tree-ring reconstruction in 2005, summer warmth exceeds warmth seen at any other time. At Sol Dav increased growth (inferred warming) that exceeds any other time begins in the 1960s. The differences in Sol Dav and OZN persist even when the chronologies are standardized in the same manner.

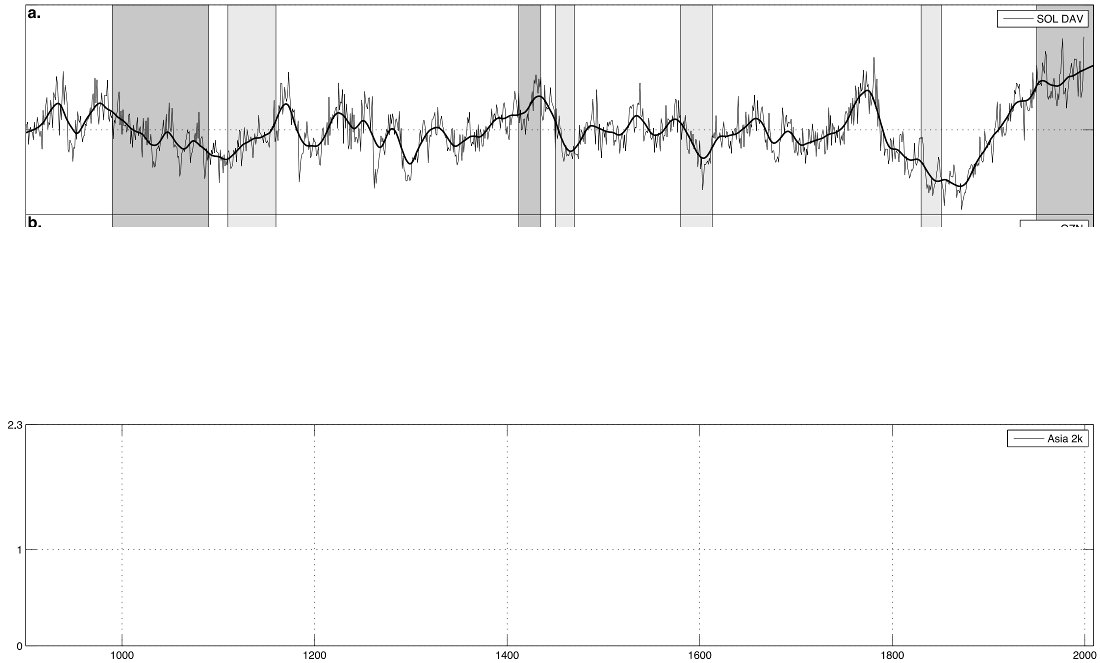

Figure 5. A comparison of Sol Dav (a.) the OZN reconstruction (b.) and the Asia 2K reconstruction (c.). CI to CV refers to cold periods, and WI to a warm period, which are consistent in all reconstructions. The y-axis for OZN is on the right, Sol Dav & Asia 2k on the left. Asia 2k y axis range is from 0 to 2.3, but OZN and Sol Dav is 0 to 2.

4.3 Volcanic influence on Mongolian Climate:

Cooling associated with explosive volcanic eruptions can influence tree growth and provides one line of evidence for the timing and magnitude of such events and their influence on the climate system (Jones et al. 1995, Briffa et al. 1998, D'Arrigo et al. 1999, D'Arrigo et al. 2013). At OZN we observe evidence of significant volcanic influence manifested as narrow rings, micro-rings, and missing rings that coincide with known eruptions. The years 934 (below average) and 935 (-2 standard deviations (SD)), the first two years of the 900s multi-decadal cold period (934-984), coincide with a massive eruption at Eldgja, Iceland (Volcanic Explosivity Index (VEI) = 6), Simkin and Siebert 1994, Stothers, et al. 1998), which may have affected temperatures for up to 8 years after the event (D'Arrigo et al. 2001b). At Sol Dav (262-1999 C.E.), the year 935 was slightly below average and frost rings were observed in the early wood during the year 938. No evidence of frost damage is found in the OZN cores or sections, although larch may be a more resistant species to frost damage then pine (Voskela 1970). A micro-ring occurs in year 1177 (-2SD) and coincides with Haku-San, in Honshu, Japan (VEI=3) and Katla in Iceland (VEI= 2, Simkin and Siebert, 1994). Another significant event, now believed to the eruption of Samalas (Indonesia) occurred in 1257 (Lavigne et al. 2013). The trees at the OZN site formed micro-rings in 1258 and for 4 years after the event; 1258 (-

1SD), 1259 (-2SD), 1260 (-2SD), 1261 (-2SD), and 1262 (-1SD), with one core missing a ring in 1259. This volcanic signal was also detected in the Sol Dav chronology; ring width was average in 1258, and below average from 1261 until 1268, with a growth low at 1262 (-2SD).

Several large-scale tropical volcanic events occurred during the LIA and are evident in the rings from the OZN site. The early 1450s eruption, believed to be in 1453 or 1454 from Kuwae in Vanuatu (Briffa et al. 1998, Gao et al. 2006), although now uncertain (Cole-Dai et al. 2013, Sigl et al. 2014), manifests as a slightly narrow ring at 1453 and a micro-ring (-1SD) in 1454. We also find a micro ring at 1458 (-1SD), which Plummer et al. (2012) argue is a second eruption from Kuwae. The 1600 eruption at Huaynaputina in Peru (VEI=6, Briffa et al. 1998) manifested as a micro-ring in 1601 (nearly -3SD) and two cores with missing rings. Micro-rings were found from 1601-1604 with the narrowest being 1603 (-3SD) and 1604 (-1SD) at Sol Dav. Narrow rings and micro-rings were found in the OZN site at 1642 (-1SD) and 1643 (-2SD), and from 1641-1644 at Sol Dav, that coincide with the 1640 eruption of Kamaga-Take, in Japan (VEI 5). The eruption of 1883 in Krakatoa, Indonesia (VEI=6, Briffa et al. 1998) manifested as a micro-ring in 1884 (nearly -3 SD) with 22 cores out of 77 missing a ring for that year. No evidence of frost rings or damage to the cells was evident in the OZN samples and Sol Dav shows only narrow ring in 1884.

Superposed Epoch Analysis provides additional support for these observations. Based on events defined using the data from Crowley et al. (2008), cooling occurred during the year of the event as well as the following year, with five subsequent years of colder temperatures (**Figure 6 a & c**). Based on the Gao et al. (2008) event list there is significant cooling the year of the event followed by one additional significant year of cooling (**Figure 6 b & d**). The shift between maximum observed cooling in Year 0 (the event year) vs Year 1 is attributable to the differences in the forcing datasets (Schmidt et al. 2012) for the maximum negative radiative forcing years, e.g. 1258 vs 1259, 1641 vs 1642, 1815 vs 1816. This observation emphasizes the importance of considering uncertainty in the forcing data (Schmidt et al. 2012, Sigl et al. 2014) when evaluating the impact of volcanic eruptions on climate using proxy records (Anchukaitis et al. 2012, D'Arrigo et al. 2013)

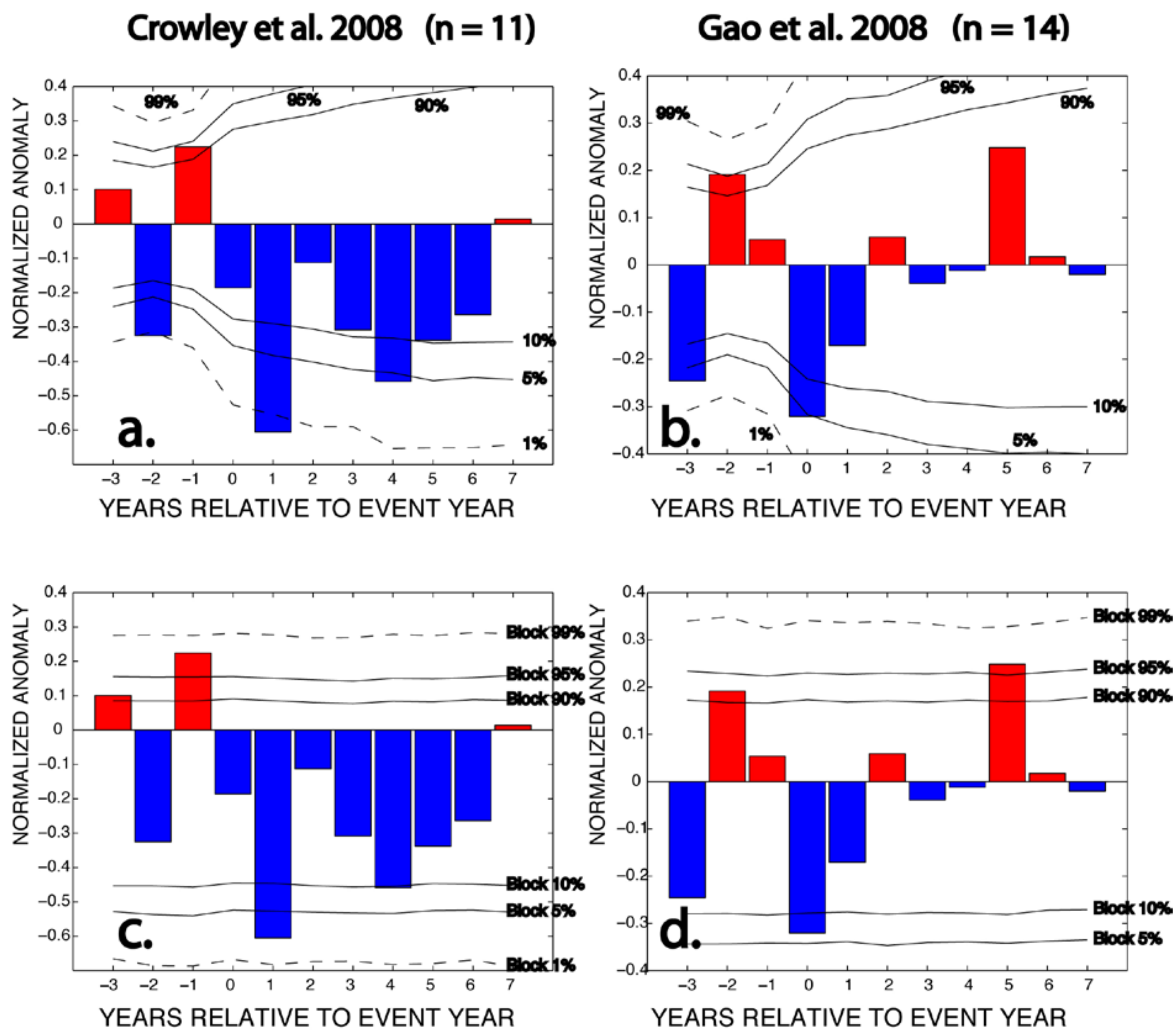

Figure 6.Results of the superposed epoch analysis (SEA) using two types of significance tests; random sampling (a & b) and block reshuffling (c & d).

4.4 Human Impacts

The OZN site used in the reconstruction here is relatively mesic, and therefore, these trees, have been immune from drought stress during periods of enhanced temperatures. However, temperature increases in recent years could have contributed to moisture deficits in many other regions of Mongolia; the summer temperatures between 1999-2002 observed in our reconstruction as a period of anomalously high temperatures could have exacerbated one of the worst droughts of the past four centuries across Mongolia (Davi et al. 2010) or past millennium in central Mongolia (Pederson et al., 2014). This drought, by means of affecting available forage resources, was also one of the contributing factors to the mass mortality of livestock seen in those years (Sheffield and Wood, 2012). Recent drought conditions in Mongolia are associated with increased grassland fires (Farukh et al., 2009), which act in conjunction with modern pressures like grassland degradation from increasing goat populations, and have resulted in the expansion of desert areas from the dry and arid southern Mongolia towards central and northern regions of the country (Liu et al., 2013). Therefore, while the trees in our study site may have benefitted from the recent warming, the deleterious impact of this temperature increase was much more widespread. Though increases in precipitation are projected in Mongolia over the next century (Christensen et al. 2013), warmer temperatures could increase evaporative demand (Sato et al. 2007, Cook et al. 2014). This effect could be detrimental to this semi-arid region in the future, which relies heavily on its agricultural economic sector.

5 Conclusion

We have described a well-verified millennial-length tree-ring reconstruction of summer temperatures from Mongolia and vicinity— the second millennial length, alpine tree-line temperature sensitive chronology from Mongolia. This reconstruction puts an unusual and unprecedented recent warming trend (since ~ the 1990s) into a long-term context for evaluation of the spatial and temporal variations of the MCA and LIA across Asia. This reconstruction also allows for evaluation of volcanic influence on Mongolian Climate.

Acknowledgements

In memory of Dr. Gordon C. Jacoby. This research was supported by the National Science Foundation under grants AGS-PRF #1137729, ATM0117442, and AGS0402474. We thank the Global Historical Climatology Network of NCDC/NOAA, Goddard Institute of Space Studies, and the Climate Research Unit for meteorological data used in this study. Field sampling was aided by students and staff of the Tree-Ring Laboratory of the Dept. of Forestry, Faculty of Biology, National University of Mongolia; and with the cooperation of the Mongolian Ministry of Nature and Environment. Lamont-Doherty Earth Observatory publication no, nnnn.

References

1. Adams JB, Mann ME, Ammann CM (2003),` Proxy evidence for an El Nino-like response to volcanic forcing. Nature 426:274–278
2. Anchukaitis, KJ, Breitenmoser P, Briffa KR, Buchwal A, Buntgen U, Cook ER, D'Arrigo RD, Esper J, Evans MN, Frank D, Grudd H, Gunnarson B, Hughes MK, Kirdyanov AV, Korner C, Krusic P, Luckman B, Melvin TM, Salzer MW, Shashkin AV, Timmreck C, Vaganov EA, Wilson R, (2012), Tree rings and volcanic cooling, Nature Geoscience, 5, 836–837, doi:10.1038/ngeo1645
3. Briffa K, Jones P, Schweingruber F, Osborn T, (1998), Influence of volcanic eruption on Northern Hemisphere temperature over the past 600 years. Nature 391, 678-682 doi :10.1038/35596
4. Chen F, Wang J, Jin L, Zhang Q, Li J, Chen J (2009) Rapid warming in mid-latitude central Asia for the past 100 years. Front. Earth Sci. China 2009, 3(1): 42–50.
5. Cole-Dai, J., D. G. Ferris, A. L. Lanciki, J. Savarino, M. H. Thiemens, and J. R. McConnell (2013), Two likely stratospheric volcanic eruptions in the 1450s C.E. found in a bipolar, subannually dated 800 year ice core record, J. Geophys. Res. Atmos., 118, 7459–7466, doi:10.1002/jgrd.50587.
6. Cook, B.I., Smerdon, J.E., Seager, R., Coats, S., (2014), Global warming and 21st century drying. Climate Dynamics: 1–21. doi:10.1007/s00382-014-2075-y
7. Cook, E. R., and Kairiukstis, L.A., 1990, Methods of Dendrochronology, Applications in the Environmental Sciences, Dordrecht: Kluwer Academic Press, 394 p.
8. Cook E, Briffa K, Jones P (1994), Spatial regression methods in dendroclimatology: A review and comparison of two techniques. International Journal of Climatology, Vol. 14, Issue 4, pp 379-402.
9. Cook ER, Briffa KR, Meko DM, Graybill DA, Funkhouser G (1995), The segment length curse in long tree-ring chronology development for paleoclimatic studies. Holocene 5:229–237

10. Cook ER, and Peters K (1997) Calculating unbiased tree-ring indices for the study of climatic and environmental change. The Holocene 7(3):359-368.

11. Cook E, Esper J, D'Arrigo R (2004), Extra-tropical Northern Hemisphere land temperature variability over the past 1000 years, Quaternary Science Reviews 23 2063–2074

12. Cook ER, Palmer J, D'Arrigo R (2002), Evidence for a 'Medieval Warm Period in a 1,100 year tree-ring reconstruction of past austral summer temperatures in New Zealand, *Geophysical Research Letters* 29 (14) 1667, 10.1029/2001GL014580

13. Cook E, Krusic P, Anchukaitis K, Buckley B, Nakatsuka T, Sano M, PAGES Asia2K Members (2013), Tree-ring reconstructed summer temperature anomalies for temperate East Asia since 800 C.E. Climate Dynamics DOI 10.1007/s00382-012-1611-x

14. Crowley, T. J., Zielinski, G., Vinther, B., Udisti, R., Kreutzs, K., Cole-Dai, J., and Castellano, E, (2008), Volcanism and the Little Ice Age, PAGES Newsletter, 16, 22–23

15. D'Arrigo, R., and G. Jacoby (1999), Northern North American tree-ring evidence for regional temperature changes after major volcanic events, Clim. Change, 41, 1–1

16. D'Arrigo R, Jacoby G, Pederson N, Frank D, Buckley B, Nachin B, Mijiddorj R, Dugarjav C (2000), Mongolian tree-rings, temperature sensitivity and reconstructions of Northern Hemisphere temperature, The Holocene 10,6, pp. 669–672.

17. D'Arrigo R, Jacoby G, Frank D, Pederson N, Cook E, Buckley B, Baatarbileg Nachin, Mijiddorj R and Dugarjav C., (2001a), 1738 years of Mongolian temperature variability inferred from a tree-ring record of Siberian pine, Geophysical Research Letters, 28:543-546.

18. D’Arrigo R, Frank D, Jacoby G, Pederson N (2001b), Spatial response to major volcanic events in or about Ad 536, 934 and 1258: frost rings and other Dendrochronological evidence from Mongolia And northern Siberia: comment on r. B. Stothers, volcanic dry fogs, climate cooling, and plague Pandemics in Europe and the middle east’, Climatic Change, 49: 239–246, 2001.

19. D’Arrigo R, Wilson R, Jacoby J (2006), On the long-term context for late twentieth century warming Journal of Geophysical Research - Atmospheres Vol. 111, No. D3, D03103, doi:10.1029/2005JD006352

20. D’Arrigo, R., R. Wilson, and K. J. Anchukaitis (2013), Volcanic cooling signal in tree ring temperature records for the past millennium, J. Geophys. Res. Atmos., 118 doi:10.1002/jgrd.50692

21. Davi N, Jacoby G, Fang K, Li J, D'Arrigo R, Baatarbileg N. Robinson. Reconstructed drought across Mongolia based on a large-scale tree-ring network: 1520-1993, (2010), Journal of Geophysical Research 15, doi:10.1029/2010JD013907

22. Diaz HF, Trig R, Hughes MK, Mann ME, Xoplaki E, Barriopedro D (2011), Spatial and temporal characteristics of climate in Medieval Times revisited, Bulletin of the American Meteorological Society DOI:10.1175/BAMS-D-10-05003.1

23. Farukh, M. A., Hayasaka, H., & Mishigdorj, O. (2009), Recent Tendency of Mongolian Wildland Fire Incidence: Analysis Using MODIS Hotspot and Weather Data. Journal of Natural Disaster Science, 31(1), 23-33.

24. Gao, C., A. Robock, S. Self, J. B. Witter, J. P. Steffenson, H. B. Clausen, M.-L. Siggaard-Andersen, S. Johnsen, P. A. Mayewski, and C. Ammann (2006), The 1452 or 1453 A.D. Kuwae eruption signal derived from multiple ice core records: Greatest volcanic sulfate event of the past 700 years, J. Geophys. Res., 111, D12107, doi:10.1029/2005JD006710.

25. Gao, C. C., Robock, A., and Ammann, C (2008), Volcanic forcing of climate over the past 1500 years: An improved ice core based index for climate models, J. Geophys. Res., 113, D23111, doi:10.1029/2008JD010239

26. Ge Q, and Wu W (2011), Climate during the MCA in China, PAGES news, Vol 19. No. 1, Eds. E Xoplaki, D Fleitmann, H Diaz, L von Gunten and T Kiefer.

27. Harris I, Jones PD, Osborn TJ, and Lister DH (2013), Updated high-resolution grids of monthly climatic observations. In press, Int. J. Climatol., Doi: 10.1002/joc.3711

28. Haurwitz MW, Brier GW (1981). A critique of the superposed epoch analysis method—its application to solar-weather relations. Mon Weather Rev 109(10):2074–2079

29. Jacoby G, D'Arrigo R, and Davaajamts T (1996), Mongolian tree rings and 20th century warming. Science 273, 771–73.

30. Jones P, Briffa K, Scheingruber F (1995), Tree-ring evidence of the widespread effects of explosive volcanic eruptions. Geophysical Research Letters 22 (11), 1333-1336, DOI: 10.1029/94GL03113

31. Juckes MN, Allen MR, Briffa KR, Esper J, Hegerl GC, Moberg A, Osborn TJ, Weber SL (2007), Millennial temperature reconstruction intercomparison and evaluation, Clim. Past, 3, 591–609,

32. Lamb HH (1965), The early medieval warm epoch and its sequel, Palaeogeography, Palaeoclimatology, Palaeoecology, 1: 13-37.

33. Lavignea F, Degeaiaʾb J, Komorowskic J, Guilletd S, Roberta V, Lahittee P, Oppenheimerf C, Stoffeldʾg M, Vidalc CM, Suronoh, PratomoI I, Wassmeraʾj P, Hajdask I, Sri Hadmokol D, and de Belizala E, (2014),

Source of the great A.D. 1257 mystery eruption unveiled, Samalas volcano, Rinjani Volcanic Complex, Indonesia

34. Liu, Y. Y., Evans, J. P., McCabe, M. F., de Jeu, R. A., van Dijk, A. I., Dolman, A. J., & Saizen, I. (2013), Changing climate and overgrazing are decimating Mongolian steppes. PloS one, 8(2), e57599.

35. Mann ME, Zhang Z, Rutherford S, Bradley RS, Hughes MK, Shindell D, Ammann C, Faluvegi G, Ni F (2009), Global signatures and dynamical origins of the little ice age and medieval climate anomaly. Science 326 (5957):1256–1260

36. Masson-Delmotte V., M. Schulz, A. Abe-Ouchi, J. Beer, A. Ganopolski, J. Gonz´alez Rouco, E. Jansen, K. Lambeck, J. Luterbacher, T. Naish, T. Osborn, B. Otto-Bliesner, T. Quinn, R. Ramesh, M. Rojas, X. Shao, and A. Timmermann. Information from paleoclimate archives. In T. Stocker, D. Qin, G.-K. Plattner, M. Tignor, S. Allen, J. Boschung, A. Nauels, Y. Xia, V. Bex, and P. Midgley, editors, Climate Change (2013), The Physical Science Basis. Contribution of Working Group I to the Fifth Assessment Report of the Intergovernmental Panel on Climate Change, pages 383–464, Cambridge, United Kingdom and New York, NY, USA, 2013. Cambridge University Press.

37. Melvin TM, Briffa KR, Nicolussi K, Grabner M (2007), Time-varying-response smoothing. Dendrochronologia 25:65-69.

38. Melvin TM and Briffa KR (2008) A ‘‘signal-free’’ approach to dendroclimatic standardization, Dendrochronologia, 26, 71–86.

39. Melvin TM and Briffa KR (2013), CRUST: Software for the implementation of Regional Chronology Standardization: Part 1. Signal-Free RCS. *Dendrochronologia* **32**, 7-20, doi: 10.1016/j.dendro.2013.06.002

40. PAGES 2K Consortium (2013), Continental-scale temperature variability during the past two millennia. *Nature Geoscience 6*, 339–346 doi:10.1038/ngeo1797

41. Pederson, N., Hessl, A. E., Baatarbileg, N., Anchukaitis, K. J., & Di Cosmo, N. (2014), Pluvials, droughts, the Mongol Empire, and modern Mongolia. *Proceedings of the National Academy of Sciences*, 111(12), 4375-4379.

42. Plummer, C.T., Curran, M.A.J., van Ommen, T.D., Rasmussen, S.O., Moy, A.D., Vance, T.R., Clausen, H.B., Vinther, B.M., Mayewski, P.A. (2012), An independently dated 2000-yr volcanic record from Law Dome, East Antarctica, including a new perspective on the dating of the 1450s CE eruption of Kuwae, Vanuatu. Climate of the Past 8, 1929e1940. http://dx.doi.org/10.5194/cp-8-1929-2012.

43. Sato, T., Kimura, F., Kitoh, A., (2007), Projection of global warming onto regional precipitation over Mongolia using a regional climate model. *Journal of Hydrology* 333: 144–154. doi:10.1016/j.jhydrol.2006.07.023

44. Schmidt, A., Carslaw, K. S., Mann, G. W., Rap, A., Pringle, K. J., Spracklen, D. V., Wilson, M., and Forster, P. M. (2012), Importance of tropospheric volcanic aerosol for indirect radiative forcing of climate, Atmos. Chem. Phys., 12, 7321-7339, doi:10.5194/acp-12-7321-2012.

45. Sheffield, J., & Wood, E. F. (2012), Drought: Past problems and future scenarios. Routledge.

46. Sigl M, McConnell JR, Toohey M, Curran M, Das S, Edwards R, Isaksson E, Kawamura K, Kipfstuhl S, Krüger K, Layman L, Maselli O, Motizuki Y, Motoyama H, Pasteris D, Severi M, 2014, Insights from Antarctica on volcanic forcing during the Common Era. *Nature Climate Change* **4**, 693–697 (2014) doi:10.1038/nclimate2293

47. Simkin, T, Siebert L, (1994), Volcanoes of the World, second ed. Geoscience Press, Tucson.

48. Stothers R, (1998), Far Reach of the Tenth Century Eldgja Eruption, Iceland, *Climatic Change* 39, 715–726.

49. Voskela, V. (1970), Frost damage on Norway Spruce, Scots Pine, Silver Birch and Siberian Larch in the forest fertilizer experimental area at Kivisuo. *Folia for. Inst. For. Fenn.*, (78).

50. Wigley TML, Briffa KR, Jones PD, (1984), On the average value of correlated time series, with applications in dendroclimatology and hydrometeorology, J. Appl. Meteorol., 23, 201–213, doi:10.1175/1520-0450(1984)023<0201:OTAVOC>2.0.CO;2.